Tropical Journal of Natural Product Research

Original Research Article

Sponge-Based Ecofriendly Antifouling: Field Study on Nets, Molecular Docking with Agelasine Alkaloids

Walter Balansa[1]*, Riyanti[2], Usy N. Manurung[4], Aprelia M. Tomasoa[1], Novriyandi Hanif[3], Frets J. Rieuwpassa[1], Till F. Schäberle[5,6]

[1]Department of Fisheries and Maritime Technology, Politeknik Negeri Nusa Utara, Kepulauan Sangihe, North Sulawesi, 95812. Indonesia
[2]Faculty of Fisheries and Marine Science, Jenderal Soedirman University, Purwokerto 53122, Indonesia
[3]Department of Chemistry, Faculty of Mathematics and Natural Sciences, IPB University (Bogor Agri-cultural University), Bogor 16680, Indonesia
[4]Department of Agribusiness, Universitas Terbuka, South Tanggerang, 15415. Indonesia
[5]Institute for Insect Biotechnology, Justus-Liebig-University of Giessen, 35392 Giessen, Germany
[6]Fraunhofer Institute for Molecular Biology and Applied Ecology (IME), Branch for Bioresources, 35392 Giessen, Germany.

ARTICLE INFO

ABSTRACT

Biofouling poses a significant threat to fisheries and maritime sectors, capable of damaging ship hulls, mariculture facilities, and marine structures. Despite the effectiveness of tributyl tin (TBT)-based antifouling in solving biofouling problems, it threatens the marine environment and human health, necessitating the exploration of ecofriendly antifouling agents. Marine sponges have evolved unique antifouling strategies that may contain potential solutions to this problem. Hence, an epoxy resin coating enriched with powder from the sponge *Agelas nakamurai* underwent field testing on polyethylene nets. Analysis of variance (ANOVA) demonstrated that nets pre-treated with 100, 200, and 300 mg/mL of the epoxy resin and sponge powder mix had a significant effect on biofouling growth (P < 0.05). Post-hoc Tukey's test indicated that the 100 mg/mL treatment significantly differed from other treatments. Since the authors previously characterized and predicted the presence of agelasines A-F (**1-6**) and agelasidine A (**7**) from the same sponge using NMR/LC-MS and MS-MS annotation, the currently studied *A. nakamurai* contains the same molecules. Molecular docking studies identified agelasines A-F and agelasidine A as promising acetylcholinesterase (AChE) inhibitors, rivaling or surpassing the AChE specific inhibitors, such as synoxazolidinones A (**8**) and C (**9**), and the antifouling agents Seanin_211 (**10**) and Irgarol_1501 (**11**). In silico ADME-T and TEST analyses on compounds **1-11** indicated that, while agelasines A-F need further optimization, agelasidine A was the most promising compound identified as potential antifouling agent in this research. This study marks the initial step in evaluating agelasines and other marine-derived molecules as eco-friendly antifouling agents

Keywords: Antifouling, acetylcholinesterase, agelasines, *Agelas nakamurai*

Introduction

The negative impacts of tributyltin-based antifouling coatings on the marine environment and human health have raised serious concerns about marine antifouling prevention.[1] Therefore, recent research has shifted towards the development of environmentally friendly antifouling solutions, using bioactive compounds sourced from and based on marine natural products.[1,2] Over the years, many compounds with antifouling properties have been discovered from marine microorganisms, e.g., α,β-unsaturated ketone from *Sarcophyton* associated fungus *Aspergillus elegans*, diindol-3-ylmethanes from *Pseudovibrio denitrificans*, butanolide from *Streptomyces albidoflavus*, and polyketides from gorgonian-derived fungus, *Aspergillus* sp., non-ribosomal peptides from seaweed associated fungus *Undaria pinnatifida*, alkaloids and terpenoids from coral and sponges.[3–6]

*Corresponding author. E mail: walterbalansa1@gmail.com
Tel: +62 821-9062-6822

Sponge, in particular, have garnered interest due to their production of bioactive compounds, which aid in biofouling prevention.[7,8] Despite the growing library of antifouling compounds, only butenolide derivatives have undergone further evaluation in field studies.[9] This is in part due to limited material supply, which remains a significant obstacle in marine drug discovery and the search for novel antifouling agents.[10-12] Preliminary investigations of crude extracts obtained from five Caribbean sponges (*Agelas tubulata, Amphimedon* sp., *Dysidea fragilis*, *Aplysina fulva*, and *Neopetrosia proxima*) have shown promise as a source of new antifouling agents.[13] Similarly, Henrikson *et al*. demonstrated antifouling activity in crude extracts and/or fractions of four marine invertebrates including two sponges, suggesting the potential use of crude extracts from marine invertebrates in antifouling studies.[14] Because sponges are also considered holobionts and contain diverse array of marine microorganisms capable of producing antifouling agents (i.e., *Alteromonas* sp., *Pseudoalteromonas piscicida*, *Bacillus licheniformis*, *Bacillus cereus*, *Bacillus* sp., *Pseudomonas fluoroscens*),[15] sponge-associated bacteria are presumably a more sustainable source of antifouling agents.[3–6]

The integration of bioinformatics to reveal new molecular targets for antifouling has streamlined such efforts; furthermore, bioinformatics prioritizes samples and can be used to generate ideas about putatively active molecules by modeling against known targets to predict their toxicity profiles.[16] Additionally, antifouling discovery can benefit from utilizing identified molecular targets such as receptors, ion channels, or enzymes, enabling the testing of both new and known molecules for new functions and/or repurposing for antifouling treatment.[17] Such

combinatorial research supports modern drug discovery and allows for the computational high-throughput screening of compounds to identify new indications.[18] Notably, the veterinary sedative medetomidine was repurposed as the antifouling solution Selektope®. through in silico analysis targeting the octopamine receptor.[19] Despite being the major target for Alzheimer diseases,[20,21] acetylcholinesterase (AChE) has recently emerged as a potential antifouling target,[22] albeit relatively unexplored.[23] AChE inhibitors have been found to prevent the settlement and attachment of barnacles such as *Balanus amphitrite* and *Pollicipes pollicipes*,[23-24] bryozoan *Bugula neritina*,[25] and ascidian *Ciona intestinalis*.[26]

Another noteworthy aspect lies in the correlation between antifouling antibacterial properties. Furthermore, the antifouling efficacy of well-established antibacterial compounds, such as *epi*-agelasine C and agelasine D against *Ulva* sp. and *Balanus improvisus* has been experimentally proven.[27] Given that the biofouling process involves the attachment of marine bacteria to submerged surfaces, followed by the formation of structured microbial communities known as biofilms, which facilitate micro and macrofouling,[1] compounds with antibacterial activity may also serve as antifouling agents.[28] However, despite the fact that many agelasine-type compounds are known to exhibit strong antibacterial activity,[29] many of these compounds have not been explored as antifouling agents.

Here, we aimed to test the antifouling potential of Sangihe sponge *Agelas nakamurai* in a field study while simultaneously performing in silico investigations on the putative binding of previously characterized and predicted Sangihe *A. nakamurai* metabolites, agelasine A and D as well as agelasine A-F and agelasidine A,[30-31] to the target AChE. This combinatorial study intends to shed light on the role of field and in silico studies for the discovery of novel antifouling agents.

Methodology

Net Preparation
The polyethylene net (Prime Grade High Density Polyethylene, AQUATEC, AquaTec Indonesia) with a mesh size of 1 inch (2.54 cm) was cut into 10x15 cm^2 pieces. Then, both the upper and undersides of each net were tied to the upper sides of the cage whereas the underside was on buoys, resembling the position of a cage floating net during fish farming.

Sponge Powder Preparation
The sponge *Agelas nakamurai* was hand-collected using self-contained underwater breathing apparatus SCUBA (Cressi, Cressi USA) from Enepahembang beach in Tahuna Sangihe Islands Regency, North Sulawesi, Indonesia, on 9 June 2019, at a depth of 7 meters. After collection, the specimen was placed in a plastic bag and transported to the laboratory at Nusa Utara Polytechnic. It was then stored at -16°C in a freezer (Aqua AQF 160w, Japan) until further use. Subsequently, the specimen, weighing 250 grams, was cut into small pieces and dried under the sun for 6 hours. The dried sponge pieces were finely ground using a blender (Philips HR2115, Phillips Indonesia), resulting in fine sponge powder.

Anti Fouling (AF) Application
Three antifouling concentrations (100, 200, and 300) mg/mL were prepared in triplicate by mixing sponge powder and epoxy resin (Durevole DPX 3100, Duravole Paint Indonesia) in the following treatments. In Treatment I, a 1:10 ratio (w/v) of sponge powder to epoxy resin was created to achieve a 100 mg/mL concentration. Treatment II and III achieved concentration of 200 mg/mL and 300 mg/mL, respectively. Treatments were then applied to polyethylene nets accordingly and air-dried for 6 hours at room temperature before installation at a mariculture's facility. In addition, untreated nets (negative control) and nets treated with epoxy resin (positive control) were also prepared in triplicate.

Data Analysis
To evaluate the effectiveness of different treatments (I, II, III alongside positive and negative controls) in preventing fouling, a systematic approach was adopted. The approach involved using the following

equation to calculate the difference between the final wet weights of all net samples and their corresponding initial wet weights:

$$Wn = Wf - Wo \ (1)$$

Where Wn signifies the net weight of biofouling affixed to nets, Wf represents the ultimate weight of the nets in addition to the biofouling affixed to the nets subsequent to being submerged in seawater for a duration of 31 days, and Wo denotes the original saturated weight of the nets in the absence of fouling, as quantified subsequent to a brief one-minute immersion in seawater before installation. Lighter nets indicated strong antifouling activity, while heavier nets indicated weaker antifouling effects. To quantitatively assess antifouling efficacy across treatments, a complete randomized design analysis of variance (ANOVA) was used, and statistical analysis was performed using the Statistical Package for Social Science (SPSS) 16.0 Program. The analysis compared average wet weights among treatment groups, providing valuable insights into the relative antifouling performances of the treatments.

In Silico Docking Experiments
The docking of all ligands (agelasines and the known acetylcholinesterase inhibitors including synoxazolidinone A and C as well as the commercial antifouling such as Seanin_211 and Irgarol_1501) inside the protein targets (6UGI) was performed using Molergo Virtual Docker 6.0. The PDB data file for the crystal structure of the target protein was retrieved from the protein databank website (http://www.rcsb.org/pdb) PDB ID: 6UGI, resolution 2.85 Å. Before docking, all errors in amino acid residues of the target protein were repaired and optimized with the neighboring residues.

The structures of all ligands were drawn using ChemDraw Ultra 12.0 to obtain 2D structures. The cdx files of all ligands and AChE inhibitors (synoxalidinones A and C) were subjected to energy minimization using Chem3D Pro and were saved in the Mol2 type format.

The selected cavities for all docking were the binding sites for acetylcholinesterase (PDB ID: 6G1U). Using Molegro Virtual Docker (MVD) 6.0, the cavities were centered at 37.09, 93.40, and 18.81 at 14 Å and run with RMDS value of <1.00 for acetylcholinesterase. We further confirmed the binding affinity of agelasines A-D, agelasidine A, synoxalidinones A and C as well as Seanin_211 and Irgarol_1501 against the acetylcholine using CB-Dock 2.[32]

In Silico ADME-T (Absorption Distribution Metabolism Excretion Toxicity) and TEST (Toxicity Estimation Software Tool) Assessments
Except for synoxalidinones A and C, the isomeric SMILES (Simplified Molecular Input Line Entry System) of all molecular structures of the ligands were obtained from PubChem for the small molecules available in the database. Because the SMILES from synoxalidinones A and C were read as errors, the structures of the molecules were first drawn using ChemDraw 12 and later converted to SMILES before being uploaded into the web tools at http://biosig.unimelb.edu.au/pkcsm/prediction for pkCSM,[33] and at http://www.swissadme.ch/ for SwissADME.[34]

Results and Discussion

Prior research has demonstrated a strong antifouling activity of agelasine, *epi*-agelasine C, and agelasine D against *Ulva* sp[35] as well as *Balanus improvisus* larvae.[27] Interestingly, Hertiani *et al.,*[36] reported that while agelasine D (**4**) inhibited the growth of *Staphylococcus epidemidis* (MIC < 0.0877 μM), it did not stop biofilm formation. In contrast, its oxime derivative showed the reverse antifouling activity, failing to inhibit the bacterial growth but succeeding to prevent biofilm formation. These investigations were conducted in laboratory settings, thereby limiting their practical application, whereas the present study evaluates antifouling potentials of epoxy resin enriched sponge powder on polyethylene nets administered at 100, 200, and 300 mg/mL for a period of 31 days in a mariculture facility, representing a real-world antifouling application. Furthermore, this study also assessed the antifouling potential of agelasines A-F (**1-6**) and agelasidine A (**7**)

against AChE enzyme in silico, underscoring the potential of agelasine-typed molecules as practical antifouling with the intention of providing valuable insights for future research and development in this field.

The results showed a significant variation in the degree of fouling organisms attaching to the treated nets versus controls (Figure 1). The negative control (treatment V) exhibited the heaviest fouling, weighing 49 g/150 cm^2 (Figure 2). In contrast, the positive control (treatment IV) was moderately settled by fouling organisms, with a weight of 36 g/150 cm^2 (Figure 2). All treated nets displayed much lower attachment of biofouling organisms, with 22g/150 cm^2 recorded for both treatment II and III, and considerably less (17 g/150 cm^2) for treatment I (Figure 2). In contrast, nets treated with the lowest concentration used in this study (treatment I) were the least fouled by fouling organisms (Figure 2). These results indicate that treatment I exhibited the most potent antifouling activity, followed by treatments II and III. Since we previously characterized agelasines A and D through NMR (Nuclear Magnetic Resonance)/Liquid Chromatography Mass Spectrometry (LC-MS)[30] and identified agelasines A-F (**1-6**) and agelasidine A (**7**) through an MS-MS based annotation approach from *Agelas nakamurai* specimen derived from Sangihe and Sitaro,[31] the observed antifouling activity was likely due to a mixture of the agelasine compounds **1-7**.

To measure the effect of the treated and untreated nets and between treatments, we conducted a randomized ANOVA data analysis on the weight of biofouling attached to the nets during the field study. The ANOVA data analysis demonstrated that treatments I-III at concentration of 100, 200 and 300 mg/mL had a significant effect on biofouling growth in comparison to both positive and negative controls ($P < 0.05$) (Table 1). To further evaluate the effectiveness of the three different treatments, we conducted a post-hoc Tukey's test, which provided further evidence that treatment I exhibited a statistically significant difference from the other treatments (Table 2). The present results align with findings from Puentes and colleagues, who reported statistically significant differences in the total coverage of fouling organisms on panels painted with extracts from sponges *Agelas tubulata*, *Holothuria glaberrima*, and *Neopetrosia proxima*.[13] However, the present results did not align with the report from Hendriksen and co-workers who documented that the antifouling activity of extracts from two sponges, one hydrozoan, and one alga when compared to the control were statistically insignificant.[14] The different coatings applied and organisms used between Hendriksen's group (gel),[14] Puentes's group (rosin resin),[13] and our present research (epoxy resin) may explain the different results obtained in these studies. Also, unlike the first two studies, the present study evaluated three different concentrations of extract/resin mixture, illuminating the lowest concentration as the most effective, which indicates that the surface characteristics of the polyethylene nets may also contain answers with respect to antifouling activity.

One explanation for this is that polyethylene nets are inherently characterized by their coarse and large surface area, which are attractive to biofouling attachment.[37,38,39] Hence, nets in the positive control (i.e. treated with epoxy resin) instead had a smooth surface and were burdened by fewer biofouling organisms at 36.6 g/150 cm^2 than the negative control with 49 g/150 cm^2 (Figure 2).
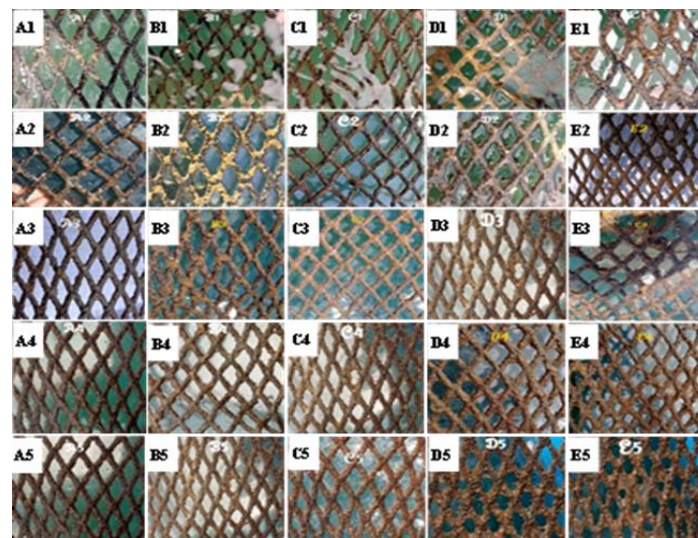

Figure 1: Polyethylene nets treated with 100 mg/mL sponge powder/epoxy resin (A1-A5, treatment I), 200 mg/mL (B1-B5, treatment II), 300 mg/mL (C1-C5, treatment III), epoxy resin (D1-D5, treatment IV), and no treatment (E1-E5, treatment V).
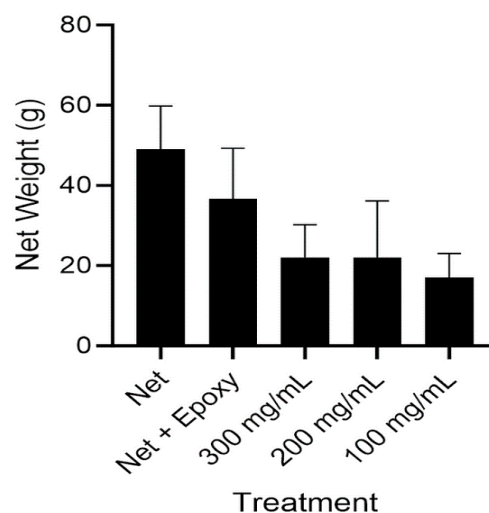
Figure 2: Biofouling weight of polyacetylene nets treated with 100 mg/mL sponge powder/epoxy resin (treatment I, 17.0 g/150 cm^2), 200 mg/mL (treatment II, 22.0 gr/150 cm^2), 300 mg/mL (treatment III, 22.0 g/150 cm^2), treatment IV or Net + epoxy (positive control, 36.66 g/150 cm^2) and negative control (Net, 49.0 g/150 cm^2).

Table 1: Statistical Data analysis

ANOVA					
Replicate	Sum of squares	Df	Mean	F	sig
Between Groups	2100,667	4	525,1667	4,551695	0,024
Within groups	1162,667	10			
Total	3263,333	14			

Table 2: Tukey Test

Tukey HSD			
Antifouling	N	Subset for alpha =	
		1	2
10%	3	17	
30%	3	22	22
20%	3	22	22
Net+epoxy	3	36.66667	36,66
Net	3		49
Sign		0.24	0,071
More for groups in homogenous subsets are displayed			

Similarly, nets treated with a more diluted antifouling solution or a less sponge powder (i.e., treatment I) featured a smoother surface and were fouled by fewer biofouling organisms compared to nets in the more concentrated antifouling treatments II (22.0 g/150 cm^2) and III (22.0 g/150 cm^2) respectively (Figure 2).

The results are consistent with earlier reports emphasizing the importance of the surface characteristics of immersed objects for the attachment of fouling organisms. For instance, Yoda *et al.* found that bacteria attached more readily to rough surfaces than to those that are smooth, as the former provides better surface attachment and adhesion for bacteria.[40] Additionally, bacteria use rough surfaces to protect themselves from shear forces, making the detachment of bacteria from the substrate difficult.[41] Indeed, rough surfaces have consistently been associated with the proliferation of bacterial colonies and biofilms, as observed for *Staphylococcus epidermidis*, *Pseudomonas aeruginosa*, and *Streptococci*.[42,43,44] Moreover, studies on titanium discs have shown that bacterial adhesion tends to be higher on surfaces measuring between 109 and 214 nm compared to smoother, grooved surfaces of less than 113 nm.[45,46]

Molecular docking studies

To further elaborate on the field study described above and earlier investigations of agelasines A and D (**1**, **4**), agelasines A-F (**1-6**) and agelasidine A (**7**) in *A. nakamurai* from Sangihe Islands,[30-31] in silico docking was employed. The objective was to evaluate the antifouling activities of agelasines A-F (**1-6**) and agelasidine A (**7**), synoxalidinones A and C (**8-9**) (known acetylcholine enzyme inhibitors), Irgarol-1501 (**10**), and Seanin-211 (**11**) (commercial antifouling agents) (Figure 3) against a novel antifouling target, AChE.[23,47]
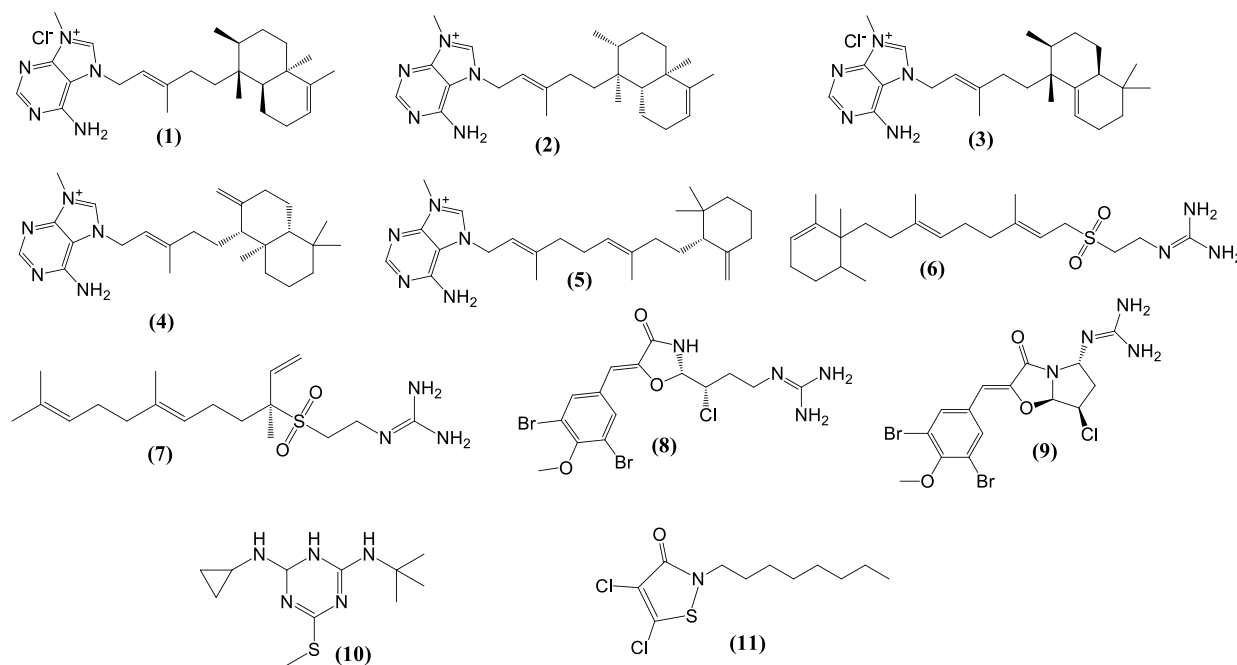

Figure 3: The structures of agelasines A-F (**1-6**), agelasidine A (**7**), synoxazolidinones A & C (**8-9**) and Irgarol_1501 (**10**) and Seanin_211 (**11**).
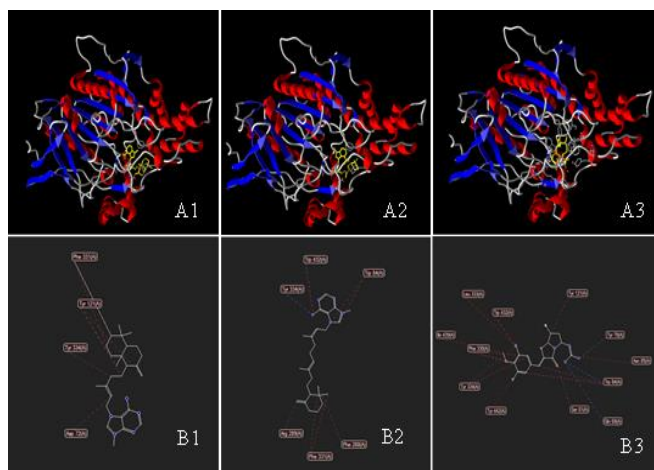
Figure 4. The binding of agelasines D, E and synoxalidinone C on the binding site of one of the dimmers 6GIU-A (A1-A3). Hydrogen bonds are denoted with blued doted lines and steric interactions with red dotted lines) (B1-B3).

The molecular docking analysis with MDV 6.0 showed strong binding of all agelasine-typed compounds against the target protein 6G1U (Figure 4, A1-A3) with all compounds showing a rerank score >150 except for Irgarol-1501 and Seanin-211 (rerank score <150) (Table 3). On the other hand, synoxazolidinone A and C showed rerank scores slightly higher or lower than all agelasines in this study (Table 3). As the strength of the binding affinity refers to the lowest binding affinity score, the highest rerank scores (-105.82, -102.19 and -96.80) kcal/mol in synoxazolidinones C (**9**), Seanine_121 (**10**), and Irgarol-1501 (**11**) respectively place them in the category of weak AChE binders. In contrast, agelasines A-C, F (**1-3**, **6**) showed slightly lower rerank scores of -108.34, -117.84, -120.0, and -116.51, indicating their moderate binding capacity to AChE. Low rerank scores of -143.39, -143.39, and -125.87 kcal/mol for agelasines D (**4**), E (**5**), and agelasidine A (**7**) categorize them as strong AChE binders (Table 3). Notably, agelasine D (**4**) exhibited three intramolecular hydrogen bonds within the cavity

of 6G1U, two of which had greater binding energy (-2.49 kcal/mol) and (-2.5 kcal/mol), and one with lesser energy (-0.27 kcal/mol). Agelasine D (**4**) also showed strong steric interactions with 6G1U at C-0, C-3, C-6, and C-30 with several amino acid of the 6G1U. Agelasine E (**5**) also exhibited steric interaction with 6G1U, where C-26 and C-30 of **5** shared interactions with two amino acid residues of 6G1U. Each of the two amino acid residues Trp84 and Trp432 shared one steric interaction with 6G1U, with moderate (1.29 strength, distance 3.09Å) and weak (0.93 strength, 3.15 Å) energy for the former and the latter (Table 3). Moreover, agelasidine A (**7**) formed four hydrogen bonding interactions with 6G1U, all of which exhibited strong affinity with Trp84, Tyr70, Gln69, Tyr121, as well as steric interactions with Trp84, Glu199, Asn85, Tyr130, Gln69, Tyr70, Tyr121, Phe330 (Table 2). Thus, of all the ligands tested in this study, agelasines D, E (**4**, **5**) and agelasidine A (**7**) showed the strongest binding affinity (Table 3).

The molecular docking was further confirmed with CB Dock-2.[32] The later docking study revealed that agelasines A-E exhibited stronger binding affinity towards 6G1U compared to the other ligands in the present investigation, with the least binding affinity being -10.5, -10.7, -10.7, and -11.8 kcal/mol for agelasines E, A, B, and D, respectively (Table 4). In contrast, agelasine A and F displayed slightly weaker binding affinity of -8.4 and -9.2 kcal/mol respectively than the specific inhibitors of AChE, synoxazolidinones A and C (binding affinity of -8.8 and -9.8 kcal/mol, respectively) but stronger than the antifouling agents Seanin-211 and Irgasol-1501 with binding affinities of -7.9 kcal/mol and -7.4 kcal/mol, respectively (Table 4).

Interestingly, despite some minor variations in the binding affinity of agelasine-type compounds, both Molegro Virtual Docker and CB-dock 2 demonstrated that all agelasine-type compounds displayed strong binding affinity to 6G1U, with agelasine D exhibiting the most potent antifouling activity (Table 3 and 4). Furthermore, all agelasine compounds in this study, except for agelasidine A (**7**), exhibited lower binding affinity than the specific AChE inhibitors synoxazolidinones A and C and the commercial antifouling compounds Seanin-211 (**10**) and Irgarol-1501 (**11**), indicating their stronger binding affinity to the target protein than both AChE inhibitors and the commercial antifouling. It is also worth noting that, except for Irgarol-1501, all compounds bound to pocket C2 chain A of the 6G1U protein target (Table 4).

Table 3: Docking results (Moldock Score, Rerank Score, H-bond, etc.,) of agelasine-type compounds, acetylcholine-specific inhibitors, and known antifouling compounds against the target protein 6G1U using MDV 6.0

Ligands	Moldock Score	Rerank score	H-bond	Interact. Amino acids	Steric Interactions	Interact. Distance (Amstrong)	Interact. Energy H-bond (Kcal/mol)
				Acetylcholinesterase (6G1U)			
Agelasine D (**4**)	−173.90	−143.79	−2.23	Tyr334, Asp72	Tyr121, Asp72, Tyr334 Trp84	2.84	−2.85
Agelasine E (**5**)	−177.80	−143.39	−3.05	Tyr334, Asp72	Asp72, Try334, Trp432, Trp84	2.74	−0.80
Agelasidine A (**7**)	−158.50	−125.87	−4.40	Trip84, Try70, Gln69, Tyr121	Trp84, Glu199, Asn85, Tyr130, Gln69, Tyr70, Tyr121, Phe330		−0.77
Synoxazolidinone-A (**8**)	−167.04	−124.25	−5.60	Ser122, Ser81, Tyr334, His440	Asn85, Trp84, Ile439, Ser81, Asp72, Trp432, Tyr334, Phe330, His440, Tyr121, Ser122	3.44,	
Agelasine C (**3**)	−158.36	−120.00	−0.02	–	Trp84, Phe330, Tyr121, Asp72, Tyr334, Gly80, Trp432	3.27, 2.63	−2.60, −2.73, −3.90
Agelasine B (**2**)	−153.36	−117.84	−2.74	Tyr334, Asp72	Tyr121,Phe331, Tyr70, Ser81,		

					Asp71, Trp84, Tyr334		
Agelasine F (**6**)	−160.02	−116.51	−7.49	Gly119, Gly118, Ser200, Tyr70, Asp72	Asn85, Trp84, Glu199, Gly118, GLy441, Aps72, Ser81	Ser122, Gly123, Gly119, Ser200, Tyr70, Tyr121	2.59, 3.15	−2.13, −1.95
Agelasine A (**1**)	−160.03	−108.34	−2.55	Ser122, Gly199	Tyr130, GLy199, Ser122, Phe290, Phe330, Tyr121, Arg289, Phe331, Ile287, Phe288	3.44	−0.77
Synoxazolidinone C (**9**)	−138.89	−105.82	−0.00	Tyr122	Tyr70, Tyr121, Phe330, Phe331, Tyr334, Ser286	2.66	−2.50
Seanin-211(**10**)	−127.90	−102.19	−0.07	–	Tyr130, His440	–	–
Irgarol-1501(**11**)	−117.61	−96.80	−0.66	His440	Glu199, His440, Ile439, Phe330, Trp84	3.45	−0.62

Table 4: Docking results of agelasines A-F (**1-6**), agelasidine A (**7**), specific inhibitors of AChE (**8-9**) and common antifouling compounds (**10-11**) against 6G1U using CB-dock 2

Ligands	Binding Capacity (Kcal/mol)	Amino acid residues
Agelasine D (**4**)	-11.8	Pocket C2, Chain A: Tyr70 Asp72 Gly80 Ser81 Glu82 Trp84 Asn85 Tyr121 Ser122 Trp279 Ser286 Ile287 Phe288 Arg289 Phe290 Phe330 Phe331 Tyr334 Gly335 Trp432 Ile439 His440 Trp442.
Agelasine C (**3**)	-10.8	Pocket C2, Chain A: Tyr70 Val71 Asp72 Gly80 Ser81 Trp84 Asn85 Gly118 Try121 Ser122 Trp279 Ser286 Ile287 Phe288 Arg289 Phe290 Phe330 Phe331 Tyr334 Gly335 Trp432 His440 Try442
Agelasine A (**1**)	-10.7	Pocket C2, Chain A: Tyr70 Val71 Asp72 Gln74 Gly80 Ser81 Glu82 Trp84 Asn85 Tyr121 Trp279 Ser286 Arg289 Phe290 Phe330 Phe331 Tyr334 Gly335 Trp432 His440 Try442
Agelasine B (**2**)	-10.7	Pocket C2, Chain A: Gln69 Try70 Val71 Asp72 Trp84 Asn85 Pro86 Gly117 Gly118 Try121 Ser122 Gly123 Trp279 Ser286 Ile287 Phe288 Arg289 Phe290 Phe330 Phe331 Tyr334 Gly335
Agelasine E (**5**)	-10.5	Pocket C2, Chain A: Tyr70 Asp72 Trp84 Asn85 Gly117 Gly118 Gly119 Tyr121 Ser122 Gly123 Ser124 Leu127 Tyr130 Glu199 Trp279 Ser286 Ile287 Phe288 Arg289 Phe290 Phe330 Phe331 Try334 Gly335 His440 Gly441 Ile444
Synoxazolidinone C (**9**)	-9.8	Pocket C2, Chain A: Gln69 Tyr70 Val71 Asp72 Ser81 Trp84 Asn85 Tyr121 Ser122 Trp279 Leu282 Ser286 Ile287 Phe288 Arg289 Phe290 Phe330 Phe331 Tyr334 Gly335
Agelasine F (**6**)	-9.2	Pocket C2, Chain A: Tyr70 Asp72 Trp84 Asn85 Gly117 Gly118 Gly119 Tyr121 Ser122 Gly123 Tyr130 Glu199 Ser200 Trp279 Leu282 Ser286 Ile287 Phe288 Arg289 Phe290 Phe330 Phe331 Tyr334 Gly335 His440
Synoxazolidinone A (**8**)	-8.8	Pocket C2, Chain A: Gln69 Tyr70 Val71 Asp72 Ser81 Trp84 Asn85 Tyr121 Ser122 Trp279 Ser286 Ile287 Phe288 Arg289 Phe290 Phe330 Phe331 Tyr334 Gly335.
Agelasidine A (**7**)	-8.4	Pocket C2, Chain A: Tyr70 Asp72 Gly80 Ser81 Glu84 Asn85 Tyr116 Gly117 Gly11 8 Tyr121 Ser122 Gly123 Leu127 Tyr130 Glu199 Ser200 Trp279 Ser286 Ile287 Phe288 Arg289 Phe290 Phe330 Phe331 Tyr334 His440 Ile444.
Seanin_211 (**10**)	-7.9	Pocket C2, Chain A: Gly80 Ser81 Trp84 Gly117 Gly118 Gly119 Tyr121 Ser122 Glu199 Ser200 Ala201 Phe288 Phe290 Phe330 Phe331 Trp432 Met436 Ile439 His440 Gly441 Tyr442
Irgarol_1501 (**11**)	-7.4	Pocket C1, Chain B: Tyr70 Val71 Asp72 Ser81 Trp84 Asn85 Gly118 Gly119 Tyr121 Ser122 Gly123 Ser200 Phe290 Phe330 Phe331 Ile439 His440 Gly441 Tyr442

In silico ADME/T and TEST Predictions
The results of the SwissADME analysis varied among ligands. All compounds exhibited favourable non-rotatable bond (nrtb) value (< 10) except for agelasidine A, which has a nrtb value of 11 (Table 5). Predicting Small Molecules Pharmacokinetics and Toxicity Properties (pkCSM) analysis also showed that agelasines A-D (**1-4**) and Seanin-211 (**10**) could penetrate the Blood Brain Barrier (BBB) while agelasines E-F (**5-6**), agelasidine A (**7**) and Irgarol-1501 (**11**) unable to (Table 6). However, along with the AChE inhibitors (**8, 9**) and commercial antifouling (**10, 11**), agelasidine A (**7**) displayed better physicochemical properties such as Log Po/w value < 4.15, resulting in all five compounds meeting the Lipinski Rule of Five (RoF) without any violations (Table 6). Whereas all ligands were potential substrates

and inhibitors of P-glycoprotein (PgP), **7**, **10** and **11** are non-PgP substrate (Table 6). Also, although toxicity, as assessed using the Loomis & Hayes criteria categorized all compounds in this study as slightly toxic (LD$_{50}$ = 2.48 to 2.88 mol/kg), the pKCSM test revealed that agelasines A-F (**1-6**) and Irgarol-1501 (**11**) displayed mutagenic, hepatotoxic, or both issues (Table 7). In contrast, agelasidine A (**7**) showed neither mutagenic nor hepatotoxic concerns (Table 7). Collectively, the results indicate a more favourable ADME-T profile for Seanin-211 (**11**) and agelasidine A (**7**) than other ligands in this study. Moreover, the Toxicity Estimation Software Tool (TEST) was employed to evaluate toxicity in accordance with the directives of the European Union. Based on the LC$_{50}$, IC$_{50}$, and IGC$_{50}$ values obtained from tests involving Fathead minnow (*Pimephales promelas*),

Tetrahymena phytiformis, and *Daphnia magna*, the compounds were classified according to their impact on aquatic life. The software calculated bioconcentration factors, toxicity categories ranging from "very toxic" for values below 1 mg/L to "harmful" for those up to 100 mg/L. Additionally, it measured bioaccumulation, acute toxicity, and mutagenicity in humans. Notably, data analysis showed that synoxazolidinone C and agelasidine A displayed harmful effects with Fathead minnow LC_{50} values of 250 mg/mL and *T. phytiformis* LC_{50} of 13 mg/mL, respectively. Agelasine A-D exhibited BCF values >100, indicating potential long-term adverse effects on aquatic organisms, whereas agelasines E-F, agelasidine A, synoxazolidinones A and C, seanin-211, and Irgarol-1501 had BCF values <100. Furthermore, the acute estimated toxicity (ATE) categorized agelasine F as fatal if swallowed (ATE = 23.81 mg/kg), synoxazolidinones C as toxic (ATE = 252.62 mg/kg), and Irgarol-1501 (**11**) as potentially harmful (ATE = 2059.46 mg/kg), with agelasines A-F, agelasidine A, synoxazolidinone A, and Seanin-211 falling into the harmful category (300 < ATE < 2000 mg/kg) (Table 3). Thus, the TEST results confirmed that agelasidine A

(**7**), synoxazolidinone A (**8**), and agelasidine A (**7**) exhibited more favourable toxicity profiles compared to other tested molecules (Table **8**).

The difference in ADME-T profiles among agelasines A-F and agelasindine A are likely attributable to structural variation within the structure class. Specifically, agelasine D contains a labdane (highlighted in red) and a 9-*N*-methyladeninium (highlighted in pink) functionalities,[49] exhibiting both Ames (mutagenicity) and hepatotoxicity issues (Figure 5). Labdane moieties in agelasines A and C are instead replaced with clerodane and halimene functionalities, respectively, resulting in a diminished hepatotoxicity while mutagenic cytotoxicity persisted (Figure 5). Similarly, monocyclic agelasines E and F exhibit mutagenic toxicity with diminished hepatotoxicity. Containing an hypotaurocyamine connected to branched diterpene instead of a 9-*N*-methyladeninium unit linked to bicyclic diterpenoid skeleton,[49] agelasidine A (**7**) has neither AMES nor hepatotoxicity issues (Figure 5).

Table 5: Physiochemical Properties of agelasines A-F (**1-6**) and agelasidine A (**7**) obtained from SwissAdme

Ligands	MiLogP	TPSA Å	Molecular Weight (MW, Da)	Hydrogen Bonding Acceptor (HBA)	Hydrogen Bonding Donor (HBD)	Non-Rotatable Bond (nrotb)
Agelasine A (**1**)	4.74	60.13	458.08	2	1	5
Agelasine B (**2**)	4.53	60.61	422.62	2	1	5
Agelasine C (**3**)	4.53	60.61	422.63	2	1	5
Agelasine D (**4**)	4.53	60.61	422.6	2	1	5
Agelasine E (**5**)	2.50	60.61	422.64	2	1	8
Agelasine F (**6**)	2.50	60.61	422.64	2	1	8
Agelasidine A (**7**)	2.87	106.9	355.54	3	2	11
Synoaxolidinone A (**8**)	1.90	111.9	496.58	4	3	6
Synoaxolidinone C (**9**)	1.90	103.2	494.57	4	2	3
Seanine_211 (**10**)	3.32	50.24	282.23	1	0	7
Irgarol_1501 (**11**)	1.33	88.5	253.37	3	2	5

Table 6: Physiochemical Properties (Log SW, log Po/w, BBB, Substrate PgP, Inhibitor CYP) of agelasines A-F (**1-6**), agelasidine A (**7**), Seanine_211 and Irgarol_1501 obtained from SwissAdme

	Physiochemical properties (SWISSADME)										
Ligand	Log *S*	Log Po/w	GI Abs. /Sol.	BBB Per.	Substrate PgP/Inhibitor CYP						LoF
					PgP	1A2	2C1	2C9	2D6	3A4	
Agelasine A (**1**)	**-5.73**	**3.22**	High/MS	Yes	Yes	No	No	No	No	No	Yes, 1V
Agelasine B (**2**)	**-5.73**	**4.23**	High/MS	Yes	Yes	No	No	No	No	No	Yes, 1V
Agelasine C (**3**)	**-5.73**	**4.24**	High/MS	Yes	Yes	No	No	No	No	No	Yes, 1V
Agelasine D (**4**)	**-5.98**	**4.33**	High/MS	Yes	Yes	No	No	Yes	No	Yes	Yes, 1V
Agelasine E (**5**)	-6.01	4.60	High/PS	No	Yes	No	No	Yes	No	Yes	Yes, 1V
Agelasine F (**6**)	-6.01	4.55	High/PS	No	Yes	No	No	Yes	No	Yes	Yes, 1V
Agelasidine A (7)	**-3.79**	**3.20**	**High/S**	**No**	**No**	**No**	**Yes**	**Yes**	**No**	**No**	**Yes, 0V**
Synoaxolidinone A (**8**)	**-5.21**	2.33	High/MS	No	Yes	No	Yes	No	Yes	No	No, 0V
Synoaxolidinone C (**9**)	-4.47	2.22	High/MS	No	Yes	No	Yes	No	No	Yes	No, 0V
Seanine_211 (**10**)	-4.83	4.37	High/MS	Yes	No	Yes	Yes	Yes	No	No	Yes, 0V
Irgarol_1501 (**11**)	-3.70	2.37	High/S	No	No	Yes	Yes	No	No	No	Yes, 0V

Note. MS = moderate solubility, PS = poorly soluble, S = soluble, 1V = 1 violation, 0V = zero violation

Table 7: Physiochemical Properties of agelasines A-F (**1-6**), agelasidine A (**7**), Seanin_211 (**10**) and Irgarol_1501 (**11**) obtained from pKCMS

| | Physiochemical properties (pKCMS) | | | | | | | | | | | | |
| | HI | BBB | Cl_{Tot} | | LD_{50} (mol/ | Hepa. | Substrate/Inhibitor CYP | | | | | | |
Ligand	(100)	Perm.	(ml/min/kg)	AMES Tox.	kg)	Tox.	2D6	3A4	1A2	C19	2C9	2D6	3A4
Agelasine D (**4**)	94.2	0.07	0.38	Yes	2.88	Yes	No	Yes	No	No	No	Yes	Yes
Agelasine C (3)	91.4	0.02	-20.4	Yes	2.46	**No**	No	No	No	No	No	No	No
Agelasine B (**2**)	94.8	0.20	0.20	Yes	2.73	Yes	No	Yes	No	No	No	Yes	Yes
Agelasine A (1)	91.8	0.02	-20.4	Yes	2.48	**No**	No	No	No	No	No	No	No
Agelasine E (**5**)	92.6	0.08	0.78	**No**	2.97	Yes	No	Yes	No	No	No	No	Yes
Agelasine F (**6**)	93.1	0.03	0.88	**No**	2.67	Yes	No	Yes	No	No	No	No	No
Agelasidine A (7)	70.4	-0.86	0.43	**No**	2.64	**No**	No	No	No	No	No	No	No
Synoxazolidinone A (**8**)	72.4	-1.36	0.43	**Yes**	2.34	**Yes**	No	Yes	No	No	No	No	No
Synoxazolidinone C (**9**)	76.2	-1.36	0.23	No	2.19	**Yes**	No	Yes	No	No	No	No	No
Seanine_211 (**10**)	90.8	0.36	0.13	**No**	2.63	**No**	No	No	Yes	Yes	No	No	No
Irgarol_1501 (**11**)	95.1	0.31	-0.95	**Yes**	2.48	**No**	No	No	No	No	No	No	No

Table 8: Toxicity of agelasines A-F (**1-6**), agelasidine A (**7**), Seanin_211 (**10**) and Irgarol_1501 (**11**) on *P. promelas*, *T. phytiformis* and *D. magna* obtained from TEST software.

Compound	SMILES Ran	Bio concentration factor (BCF)	*Pimephales promelas* (mg/mL)	*Tetrahymena phytiformis* (mg/L)	*Daphnia magna* (mg/L)	Oral (mg/kg)	Red
Agelasine A (**1**)	[H]C12CCC=C(C)C2(C)CCC(C)C1(C)CCCC(=CC[N+]3=CN(C=4N=CN=C(N)C43)C)C	192.31	0.45	NA	0.44	610	
Agelasine B (**2**)	C[C@@H]1CC[C@@]2([C@@H]([C@@]1(C)CC/C(=C/CN3C=[N+](C4=NC=NC(=C43)N)C)/C)CCC=C2C)C	192.77	0.45	NA	0.44	610.63	
Agelasine C (**3**)	N=1C=NC2=C(C1N)N(C=[N+]2C)CC=C(C)CCC3(C4=CCCC(C)(C)C4CCC3C)C	196.49	0.41	NA	0.41	607.23	
Agelasine D (**4**)	N=1C=NC2=C(C1N)N(C=[N+]2C)CC=C(C)CCC3C(=C)CCC4C(C)(C)CCCC34C	139.74	0.34	NA	0.49	614.83	
Agelasine E (**5**)	N=1C=NC2=C(C1N)N(C=[N+]2C)CC=C(C)CCC=C(C)CCC3C(=C)CCCC3(C)C	59.97	0.26	NA	2.56	527.91	
Agelasine F (**6**)	C[C@@H]([C@@]1(CC/C(C)=C/CC[C@](C=C)(S(=O)(CC/N=C(N)\N)=O)C)C)CCC=C1C=O	3.16	0.09	1.76	0.59	23.81	
Agelasidine A (**7**)	O=S(=O)(CCN=C(N)N)C(C=C)(C)CCC=C(C)CCC=C(C)C	7.42	0.16	11.3	0.51	342.51	
Synoxazolidinone A (**8**)	COC1=C(C=C(C=C1Br)/C=C\2/C(=O)N[C@@H](O2)[C@H](CCN=C(N)N)Cl)Br	1.9	0.15	3.49	0.51	349.15	

Synoxazolidinone C (**9**)	COC1=C(C=C(C=C1Br)/C=C\2/C(=O)N3[C@H](C[C@@H]([C@@H]3O2)Cl)N=C(N)N)Br	4.85	252.62	3.92	1.04	252.62
Seanin_211 (**10**)	ClC1=C(Cl)SN(CCCCCCCC)C1=O	37.44	0.13	7.3	2.98	767.55
Irgarol_1501 (**11**)	N=1C(=NC(=NC1NC2CC2)NC(C)(C)C)SC	19.29	5.42	NA	9.4	2059.46

Thus, the field study has provided empirical evidence that supports the practical application of sponge powder as a potent antifouling agent. The treated nets showed significantly lower levels of settlement by biofouling organisms than the controls. Statistical analysis confirmed that treatment I (100 mg/mL) demonstrated the strongest antifouling activity. These findings not only validate the efficacy of agelasine-type compounds in real-world conditions but also underscore the significance of surface characteristics in biofouling prevention Consequently, restricting the use of powdered materials as antifouling agents for polyethylene nets is crucial in reducing surface roughness and, in turn, decreasing the attachment of fouling organisms.

Additionally, the potential of agelasines A-F as antifouling agents was demonstrated through molecular docking of all ligands on AChE using Molergo Virtual Docker and CB-dock 2. The binding affinities of the sponge-derived molecules were found to be stronger against AChE in comparison to the specific acetylcholine esterase inhibitors (synoxazolidinones A and C) and commercial antifouling agents (Seanin-211 and Irgarol-1501), indicating their efficacy as antifouling agents. This discovery not only provides new insights into the antifouling activity of agelasine-typed compounds but also confirms the previous reports of the antibacterial and antifouling activity of agelasine D, which was found to be effective against *Balanus improvisus* and also showed antibacterial effects against both, Gram-negative and Gram-positive bacteria.[30] This finding aligns with report from Do and coworkers who reported that daily exposure to the commercial antifouling Seanine_211 (DCOIT) at 100 ng/L,[50] resulted in retardation in morphometric parameters and significant inhibition of AChE activity after 4-week treatment of the fouling organism, marine mysid

(*Meomysis awatschensis*). The authors claimed that the inhibition is related to the impairment of the cholinergic system, which may affect the growth of the mysid. Similarly, Lee *et al*., reported that TBT, diuron and Irgarol-1505 showed antifouling activity and toxic cholinergic effect on nauplii through AChE inhibition.[51] Furthermore, it was also reported that compounds that inhibited AChE were capable of inhibiting invertebrate larval settlement,[23] suggesting a correlation between AChE inhibition and antifouling activities to prompt further investigations of the enzyme as an emerging target for the discovery of new antifouling agents.

The analysis of ADMET-T for ligands offers valuable insights into the potential of antifouling agents and their safety profiles. While agelasines A-F and agelasidine A showed strong binding affinity against the antifouling target acetylcholine esterase, only agelasidine A (**7**) exhibited favourable ADME-T properties, while others necessitated further optimization. The presence of specific moieties in the agelasine compounds has been shown to improve ADME-T profiles, (e.g., agelasidine A in this study), or to induce different antifouling activities (i.e., preventing microfouling and biofilm formation in agelasine D and its oxime derivative).[36] This also underscores the importance of structurally modifying or simplifying the diverse agelasine-type compounds to discover new antifouling agents from this structural class. This approach is akin to Polanski's technique, which involves trimming unnecessary molecular components, known as "molecular obesity," to enhance pharmacokinetic profiles, reduce side effects, and increase the market success of drug leads.[52] Eribulin mesylate, fingolimod, vorinostat, and devazepide are examples of drugs that owe their success to this technique.[53]
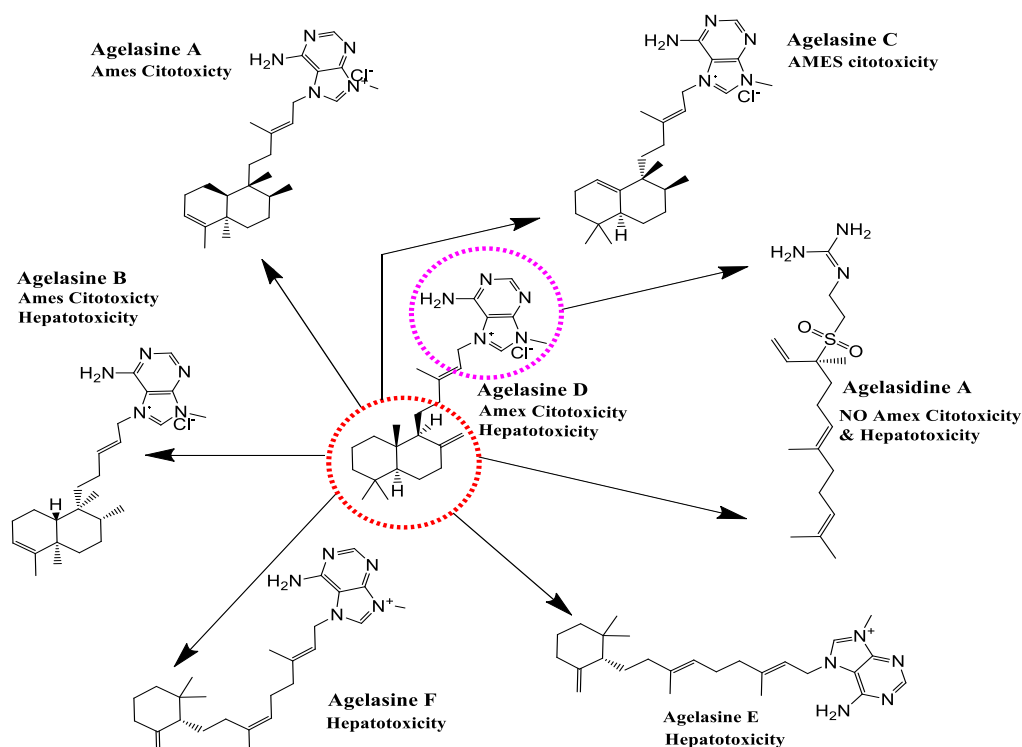

Figure 5. The various toxicities of agelasine-typed compounds due to their different molecular structures with agelasine D responsible for mutagenic effects (Ames) and hepatotoxicity, agelasine A (Ames toxicity), agelasine B (Ames cytotoxicity and hepatotoxicity), agelasine E (hepatotoxicity), agelasine F (hepatotoxicity)

The application of computational technology provides numerous benefits for the discovery of eco-friendly antifouling agents. Although the antifouling activity of agelasine D has already been reported, this activity was new for the other molecules tested in this study. Additionally, the in silico analysis and field study each demonstrated that molecules with antibacterial properties, such as agelasine B and D,[30] as well as agelasines A-F and agelasidine A,[31] are likely to exhibit antifouling activities. This finding aligns with the biofouling attachment theory, which suggests that bacteria initiate attachment on surfaces, form biofilm, and then attract other microorganisms, such as invertebrate larvae or algae spores, to attach and metamorphose into macrofouling.[11,13]

Despite the longstanding problem of material supply issues in natural product-based antifouling discovery,[54] the use of unrefined extracts or combinations of compounds holds potential for practical implementation.[13] This, in turn, contributes to the pressing need for environmentally safe antifouling solutions. Additionally, many sponges are thought to remain unaffected by biofouling, since they contain bioactive metabolites.[7,8] Because many of these molecules present in the holobiont are not biosynthesized by the sponge itself but may be derived from symbiotic microorganisms or from their interactions,[55] it is crucial to not only focus on sponge powder or extracts but also on sponge microbial symbionts as alternative and sustainable source of novel antifouling agents.

The field study was conducted within a limited timeframe employing sponge powder. Despite the recent application of compound mixture in antifouling studies,[13] it is critical to assess the antifouling activity of agelasine-type compounds independently. As such, our future research endeavours will replicate the same study utilizing pure compounds for an extended period of time (6-12 months), in order to comprehensively understand the antifouling potential of the putative antifouling agent(s). Moreover, forthcoming investigations should address the ADMET-T concerns of agelasines through the implementation of structural simplification analysis to optimize their antifouling potential.[53] Furthermore, since the recent findings were derived from a predictive study in silico, further optimized in silico and field studies pertaining to the present putative antifouling agents are warranted to confirm the current outcomes.

Finally, biofouling is a complex phenomenon, which requires multidisciplinary approaches.[56] Therefore, in addition to the chemistry of sponges or their symbiotic microorganisms, future studies should incorporate additional factors such as surface charge, surface wettability, roughness, topography, stiffness, and a combination of these properties to comprehensively evaluate antifouling activity.[57] Additionally, the exploration of emerging antifouling targets like AChE are of equal importance.[47] These approaches can help the discovery of novel, effective, environmentally friendly, and sustainable antifouling lead compounds.

Conclusion

In summary, there is a pressing need for the discovery of eco-friendly antifouling agents to combat biofouling threats in the fisheries and maritime sectors. The results of this field study indicate that a treatment of 100 mg/mL exhibited the most significant antibiofouling effect, since likely effects of the sponge-derived compounds and the surface of the coating has to be considered. Because we previously characterized agelasine A and D and predicted the presence of agelasines A-F and agelasidine A with the use of NMR/LC-MS and metabolomics, respectively , it is assumed that the antifouling activity of the sponge powder was due to either agelasine A-F, agelasidine F or a combination of the two. Molecular docking analysis revealed that agelasine-type compounds could serve as promising antifouling agents due to their strong binding to AChE, which was comparable or superior to AChE-specific inhibitors (i.e., synoxazolidinones A and C), and commercial antifouling agents (e.g., Seanin-211 and Irgarol-1501). Although ADME-T analysis revealed that, most agelasine-typed compounds require further optimisation, agelasidine A showed promising ADME-T parameters in this study. To validate these findings, additional field studies focusing on agelasidine A as a pure compound are necessary. This research marks a crucial initial step in exploring marine-derived molecules as environmentally friendly antifouling agents, holding future practical applications in the field. The observed effects and promising parameters warrant further investigation, paving the way for future advancements in sustainable antifouling solutions.

Conflict of Interest

The authors declare no conflict of interest.

Authors' Declaration

The authors hereby declare that the work presented in this article is original and that any liability for claims relating to the content of this article will be borne by them.

Acknowledgments

References

1. Gomez, BJ. Marine natural products: a promising source of environmentally friendly antifouling agents for the maritime industries. Front. Mar. Sci. 2022;9:858757. doi.org/10.3389/fmars.2022.858757.

2. Liu LL, Wu CH, Qian PY. Marine natural products as antifouling molecules–a mini-review (2014–2020). Biofoul. 2020;36(10):1210-1226. doi:10.1080/08927014.2020.1864343

3. Qi SH, Ma X. Antifouling compounds from marine invertebrates. Mar Drugs. 2017;15(9). doi:10.3390/md15090263

4. Qian PY, Li Z, Xu Y, Li Y, Fusetani N. Mini-review: Marine natural products and their synthetic analogs as antifouling compounds: 2009–2014. Biofoul. 2015;31(1):101-122. doi:10.1080/08927014.2014.997226

5. Wang KL, Xu Y, Lu L, Li Y, Han Z, Zhang J, Shao CL, Wang CY, Qian PY. Low-toxicity diindol-3-ylmethanes as potent antifouling compounds. Mar Biotechnol. 2015;17(5):624-632. doi:10.1007/s10126-015-9656-6

6. Wang KL, Wu ZH, Wang Y, Wang CY, Xu Y. Mini-review: Antifouling natural products from marine microorganisms and their synthetic analogs. Mar Drugs. 2017;15(9):1-21. doi:10.3390/md15090266

7. Prieto IM, Paola A, Pérez M, García M, Blustein G, Schejter L, Palermo JA. Antifouling diterpenoids from the sponge *Dendrilla antarctica*. Chem Biodivers. 2022;19(2):2003-2005.doi: doi.org/10.1002/cbdv.202100618.

8. Sánchez LI, Hernández GCJ, Muñoz, OM, Hellio C. Biomimetic approaches for the development of new antifouling solutions: Study of incorporation of macroalgae and sponge extracts for the development of new environmentally-friendly coatings. Int J Mol Sci. 2019;20(19):1-18. doi:10.3390/ijms20194863.

9. Chiang HY, Cheng J, Liu X, Ma C, Qian PY. Synthetic analogue of butenolide as an antifouling agent. Mar Drugs. 2021;19(9):1-12. doi:10.3390/md19090481

10. Liang X, Luo D, Luesch H. Advances in exploring the therapeutic potential of marine natural products. Pharmacol Res. 2019;147:104373. doi:10.1016/j.phrs.2019.104373

11. Fusetani N. Antifouling marine natural products. Nat Prod Rep. 2011;28(2):400-410. doi:10.1039/c0np00034e

12. Xu Y, He H, Schulz S, Liu X, Fusetani N, Xiong H, Xiao X, Qian PY. Potent antifouling compounds produced by marine

Streptomyces. Bioresour Technol. 2010;101(4):1331-1336. doi:10.1016/j.biortech.2009.09.046

13. Puentes C, Carreño K, Santos-Acevedo M, Gómez-León J, García M, Pérez M, Stupak M, Blustein G. Anti-fouling paints based on extracts of marine organisms from the Colombian Caribbean. Cienc y Tecnol buques. 2014;8(15):75. doi:10.25043/19098642.105.

14. Henrikson AA, Pawlik JR. A new antifouling assay method: results from field experiments using extracts of four marine organisms. J Exp Mar Bio Ecol. 1995;194(2):157-165. doi:10.1016/0022-0981(95)00088-7

15. Satheesh S, Ba-Akdah MA, Al-Sofyani AA. Natural antifouling compound production by microbes associated with marine macroorganisms — A review. Electron J Biotechnol. 2016;21(2015):26-35. doi:10.1016/j.ejbt.2016.02.002

16. Pereira F, Aires-de-Sousa J. Computational methodologies in the exploration of marine natural product leads. Mar Drugs. 2018;16(7). doi:10.3390/md16070236

17. Hellio C, Yebra D. Advances in marine antifouling coatings and technologies. Woodhead Publishing Limited, Cambridge. 2009. 748 p.

18. Agamah FE, Mazandu GK, Hassan R, Bope CD, Thomford NE, Ghansah A, Chimusa ER. Computational/in silico methods in drug target and lead prediction. Brief Bioinform. 2020;21(5):1663-1675. doi:10.1093/bib/bbz103

19. Lind U, Rosenblad MA, Frank LH, Falkbring S, Brive L, Laurila JM, Pohjanoksa K, Vuorenpää A, Kukkonen JP, Gunnarsson L, Scheinin M.l. Octopamine receptors from the barnacle Balanus improvisus are activated by the α2-adrenoceptor agonist medetomidine. Mol Pharmacol. 2010;78(2):237-248. doi:10.1124/mol.110.063594

20. Dhanjal JK, Sharma S, Grover A, Das A. Use of ligand-based pharmacophore modeling and docking approach to find novel acetylcholinesterase inhibitors for treating Alzheimer's. Biomed Pharmacother. 2015;71:146-152. doi:10.1016/j.biopha.2015.02.010

21. Akıncıoğlu H, Gülçin İ. Potent Acetylcholinesterase inhibitors: potential drugs for Alzheimer's disease. Mini Rev Med Chem. 2020;20(8):703-715.

22. Arabshahi HJ, Trobec T, Foulon V, Hellio C, Frangež R, Sepčić K, Cahill P, Svenson J. Using Virtual AChE Homology screening to identify small molecules with the ability to inhibit marine biofouling. Front Mar Sci. 2021;8:1-12. doi:10.3389/fmars.2021.762287

23. Almeida JR, Moreira J, Pereira D, Pereira S, Antunes J, Palmeira A, Vasconcelos V, Pinto M, Correia-da-Silva M, Cidade H. Potential of synthetic chalcone derivatives to prevent marine biofouling. Sci Total Environ. 2018;643:98-106. doi:10.1016/j.scitotenv.2018.06.169

24. Blihoghe D, Manzo E, Villela A, Cutignano A, Picariello G, Faimali M, Fontana A. Evaluation of the antifouling properties of 3-alyklpyridine compounds. Biofoul. 2011;27(1):99-109. doi:10.1080/08927014.2010.542587

25. Yu X, Yan Y, Gu JD. Attachment of the biofouling bryozoan Bugula neritina larvae affected by inorganic and organic chemical cues. Int Biodeterior Biodegrad. 2007;60(2):81-89. doi:10.1016/j.ibiod.2006.12.003

26. Mansueto V, Cangialosi MV, Arukwe A. Acetylcholinesterase activity in juvenile Ciona intestinalis (Ascidiacea, Urochordata) after exposure to tributyltin. Caryolog. 2012;65(1):18-26. doi:10.1080/00087114.2012.678082

27. Sjögren M, Dahlström M, Hedner E, Jonsson PR, Vik A, Gundersen LL, Bohlin L. Antifouling activity of the sponge metabolite agelasine D and synthesised analogs on Balanus improvisus. Biofoul. 2008;24(4):251-258. doi:10.1080/08927010802072753

28. Tadesse, M., Svenson, J., Sepčić, K., Trembleau, L., Engqvist, M., Andersen, J.H., Jaspars, M., Stensvåg, K. and Haug, T. Isolation and synthesis of pulmonarins A and B,

acetylcholinesterase inhibitors from the colonial ascidian Synoicum pulmonaria. J Nat Prod. 2014;77(2):364-369. doi:10.1021/np401002s

29. Chu MJ, Li M, Ma H, Li PL, Li GQ. Secondary metabolites from marine sponges of the genus Agelas: A comprehensive update insight on structural diversity and bioactivity. RSC Adv. 2022;12(13):7789-7820. doi:10.1039/d1ra08765g

30. Balansa W, Wodi SIM, Rieuwpassa FJ, Ijong FG. Agelasines B, D and antimicrobial extract of a marine sponge Agelas sp. From Tahuna Bay, Sangihe Islands, Indonesia. Biodiv. 2020;21(2):699-706. doi:10.13057/biodiv/d210236

31. Riyanti, Marner M, Hartwig C, Patras MA, Wodi SI, Rieuwpassa FJ, Ijong FG, Balansa W, Schäberle TF. Sustainable low-volume analysis of environmental samples by semi-automated prioritization of extracts for natural product research (SeaPEPR). Mar Drugs. 2020;18(649):1-15.

32. Liu Y, Grimm M, Dai W tao, Hou M chun, Xiao ZX, Cao Y. CB-Dock: a web server for cavity detection-guided protein–ligand blind docking. Acta Pharmacol Sin. 2020;41(1):138-144. doi:10.1038/s41401-019-0228-6

33. Pires DEV, Blundell TL, Ascher DB. pkCSM: Predicting small-molecule pharmacokinetic and toxicity properties using graph-based signatures. J Med Chem. 2015;58(9):4066-4072. doi:10.1021/acs.jmedchem.5b00104

34. Daina A, Michielin O, Zoete V. SwissADME: A free web tool to evaluate pharmacokinetics, drug-likeness and medicinal chemistry friendliness of small molecules. Sci Rep. 2017;7(March):1-13. doi:10.1038/srep42717

35. Hattori T, Adachi K, Shizuri Y. New agelasine compound from the marine sponge Agelas mauritiana as an antifouling substance against macroalgae. J Nat Prod. 1997;60(4):411-413. doi:10.1021/np960745b

36. Hertiani T, Edrada-Ebel R, Ortlepp S, van Soest RW, de Voogd NJ, Wray V, Hentschel U, Kozytska S, Müller WE, Proksch P. From anti-fouling to biofilm inhibition: New cytotoxic secondary metabolites from two Indonesian Agelas sponges. Bioorganic Med Chem. 2010;18(3):1297-1311. doi:10.1016/j.bmc.2009.12.028

37. Hodson SL, Lewis TE, Burke CM. Biofouling of fish-cage netting: Efficacy and problems of in situ cleaning. Aquaculture. 1997;152(1-4):77-90. doi:10.1016/S0044-8486(97)00007-0

38. Hudson S, Lewis TE, Burke CM. In situ quantification of fish-cage fouling by underwater photography and image analysis. Biofoul. 1995;9(2):145-151. doi:10.1080/08927019509378298

39. Kartal GE, Sarışık AM. Providing antifouling properties to fishing nets with encapsulated econea. J Ind Text. 2022;5:7569S-7586S. doi:10.1177/1528083720920568

40. Yoda I, Koseki H, Tomita M, Shida T, Horiuchi H, Sakoda H, Osaki, M. Effect of surface roughness of biomaterials on Staphylococcus epidermidis adhesion. BMC Microbiol. 2014;14(1):1-7. doi:10.1186/s12866-014-0234-2

41. Bollen CML, Papaioanno W, Van Eldere J, Schepers E, Quirynen M, Van Steenberghe D. The influence of abutment surface roughness on plaque accumulation and peri-implant mucositis. Clin Oral Implants Res. 1996;7(3):201-211. doi:10.1034/j.1600-0501.1996.070302.x

42. Abdalla MM, Ali IA, Khan K, Mattheos N, Murbay S, Matinlinna JP, Neelakantan P. The Influence of surface roughening and polishing on microbial biofilm development on different ceramic materials. J Prosthodont. 2021;30(5):447-453. doi:10.1111/jopr.13260

43. Nogueira RD, Silva CB, Lepri CP, Palma-Dibb RG, Geraldo-Martins VR. Evaluation of surface roughness and bacterial adhesion on tooth enamel irradiated with high intensity lasers. Braz Dent J. 2017;28(1):24-29. doi:10.1590/0103-6440201701190

44. Yu B, Chen X, Li J, Qu Y, Su L, Peng Y, Huang J, Yan J, Yu Y, Gu Q, Zhu Z. Stromal fibroblasts in the microenvironment

of gastric carcinomas promote tumor metastasis via upregulating TAGLN expression. BMC Cell Biol. 2013;14(1):1. doi:10.1186/1471-2121-14-17

45. Xing R, Lyngstadaas SP, Ellingsen JE, Taxt-Lamolle S, Haugen HJ. The influence of surface nanoroughness, texture and chemistry of TiZr implant abutment on oral biofilm accumulation. Clin Oral Implants Res. 2015;26(6):649-656. doi:10.1111/clr.12354

46. Yao WL, Lin JC, Salamanca E, Pan YH, Tsai PY, Leu SJ, Yang KC, Huang HM, Huang HY, Chang WJ. Er, Cr. Laser Performance Improves Biological. Mater. 2020;13(1):1-14.

47. Gaudêncio SP, Pereira F. Predicting antifouling activity and acetylcholinesterase inhibition of marine-derived compounds using a computer-aided drug design approach. Mar Drugs. 2022;20(2). doi:10.3390/md20020129

48. Hayes AW, Loomis TA. Loomis's essentials of toxicology. (4th ed.). New York: Academic Press; 1996, 282 p.

49. Chu MJ, Li M, Ma H, Li PL, Li GQ. Secondary metabolites from marine sponges of the genus *Agelas*: a comprehensive update insight on structural diversity and bioactivity. RSC adv. 2022;12(13):7789-820

50. Do JW, Haque MN, Lim HJ, Min BH, Lee DH, Kang JH, Kim M, Jung JH, Rhee JS. Constant exposure to environmental concentrations of the antifouling biocide Sea-Nine retards growth and reduces acetylcholinesterase activity in a marine mysid. Aquat Toxicol. 2018;205:165-173. doi:10.1016/j.aquatox.2018.10.019

51. Lee DH, Eom HJ, Kim M, Jung JH, Rhee JS. Non-target effects of antifouling agents on mortality, hatching success, and acetylcholinesterase activity in the brine shrimp Artemia salina. Toxicol Environ Health Sci. 2017;9(3):237-243. doi:10.1007/s13530-017-0326-0

52. Polanski J, Bogocz J, Tkocz A. The analysis of the market success of FDA approvals by probing top 100 bestselling drugs. J Comput Aided Mol Des. 2016;30(5):381-389. doi:10.1007/s10822-016-9912-5

53. Wang S, Dong G, Sheng C. Structural simplification: an efficient strategy in lead optimization. Acta Pharm Sin B. 2019;9(5):880-901. doi:10.1016/j.apsb.2019.05.004

54. Pereira F. Have marine natural product drug discovery efforts been productive and how can we improve their efficiency? Exp. Op. Drug Dis. 2019;14(8):717-22.

55. Indraningrat AAG, Smidt H, Sipkema D. Bioprospecting sponge-associated microbes for antimicrobial compounds. Mar Drugs. 2016;14(5):1-66. doi:10.3390/md14050087

56. Qiu H, Feng K, Gapeeva A, Meurisch K, Kaps S, Li X, Yu L, Mishra YK, Adelung R, Baum M. Functional polymer materials for modern marine biofouling control. Prog Polym Sci. 2022;127. doi:10.1016/j.progpolymsci.2022.101516

57. Zheng S, Bawazir M, Dhall A, Kim HE, He L, Heo J, Hwang G. Implication of surface properties, bacterial motility, and hydrodynamic conditions on bacterial surface sensing and their initial adhesion. Front Bioeng Biotechnol. 2021;9:1-22. doi:10.3389/fbioe.2021.643722